Microelectronic Engineering 112 (2013) 269–272

Contents lists available at SciVerse ScienceDirect

Microelectronic Engineering

journal homepage: www.elsevier.com/locate/mee

Development of MEMS integrated into TEM setup to monitor shear deformation, force and stress for nanotribology

Takaaki Sato [a,*], Laurent Jalabert [b], Hiroyuki Fujita [a]

[a] Institute of Industrial Science, University of Tokyo, Meguro-ku, Tokyo 153-8505, Japan
[b] LIMMS/CNRS-IIS Institute of Industrial Science, University of Tokyo, Meguro-ku, Tokyo 153-8505, Japan

ARTICLE INFO

Article history:
Available online 6 April 2013

Keywords:
MEMS
TEM
Friction
Actual contact area

ABSTRACT

The observation of nanoscale shear deformations is a significant step toward understanding the mechanisms of friction and lubrication, because these processes depend on the collective behavior of nanoscale junctions on sliding surfaces. We have developed a MEMS-in-TEM setup that enabled us to observe shear deformation and measure shear force, displacement and shear stress at the nanoscale level. Our experimental results reveal that the shear strength increases in the nano-meter range and indicate that the frictional coefficient may increase when the actual contact area is composed of nanojunctions rather than micro-sized junctions.

1. Introduction

Nanotribology, including nanoscale wear and friction, is an important concern for the reliability of micro- and nanodevices (MEMS and NEMS). Digital micromirror devices, as well as RF MEMS switches and multi-probes AFMs, operate with mid- or high-frequency contacts between two micro-areas of the device, leading to damage induced by tribological effects [1]. The behavior of multiple contacts between two surfaces is still not understood and is difficult to model from an atomistic point of view because it involves randomly formed asperities on both surfaces. Understanding nanotribology through a model that assumes two single asperities composed from the same material is, therefore, a relevant simplification or discretization of a complex problem observed at the micro-scale.

Amontons' friction law, which quit accurately describes the friction between two macroscale objects in contact, states that the frictional force F is proportional to the normal force N with an empirical frictional coefficient μ. The "adhesion model" later proposed by Bowden and Taber [2] is based on the notion of real contact area rather the apparent contact area as the result of multiple contacts between asperities. The "adhesion model" states that the friction phenomenon is the sum of the shear deformation of the individual asperities that form the real contact area.

The adhesion force between two asperities is strongly dependent on the quality/purity of the contact area interface (e.g., the presence of uncontrolled contamination, or lubricants) and the environment (dry or wet conditions). Feynman [3] stipulated that friction forces originate from viscous forces between atoms acting incoherently across a sliding interface and can be lowered by reducing the viscous forces through operating under (ultra-high) vacuum conditions.

However, from a practical point of view, ultra-high vacuum conditions enhance atomic rearrangement to form commensurate interfaces, yielding a higher frictional coefficient. As an example, the so-called "cold welding" process [1,4], which is observed when two clean metal surfaces are placed in contact in UHV, is based on atom diffusion to the interface (driven by the strong adhesion force) to reduce the number of atoms exposed to the vacuum and maximize the metal–metal contact area. Such cold-welded metallic contacts in UHV can be elongated to form atomic chains that have been intensively studied, especially to measure the quantum of electrical conductance [5–10]. Mechanical testing in the longitudinal direction has also been performed [11,12].

Maintaining an incommensurate interface in dry conditions while reducing nanoscale friction forces appears to be a "nano-lubricity" challenge. Therefore, understanding the nano-lubricity mechanism requires a dynamic observation of frictional interfaces under high-vacuum conditions while sliding. One of the most suitable engineering techniques to dynamically observe incommensurate "sliding" interfaces relies on combining a conventional atomic force microscope (AFM) or a frictional force microscopes (FFM) with a transmission electron microscope [13,14]. Although the resulting holder prototype is expensive and not versatile in design, its main merit relies on the two independently made opposing tips that can be pre-coated with different materials. The combined piezo-driven tip (tungsten) and AFM tip in the TEM brings new insight into studying nanoscale wear and provides evidence for how

* Corresponding author. Tel.: +81 3 5452 6249; fax: +81 3 5452 6250.
E-mail addresses: takaakis@iis.u-tokyo.ac.jp (T. Sato), fujita@iis.u-tokyo.ac.jp (H. Fujita).

0167-9317/$ - see front matter © 2013 Elsevier B.V. All rights reserved.
http://dx.doi.org/10.1016/j.mee.2013.03.156

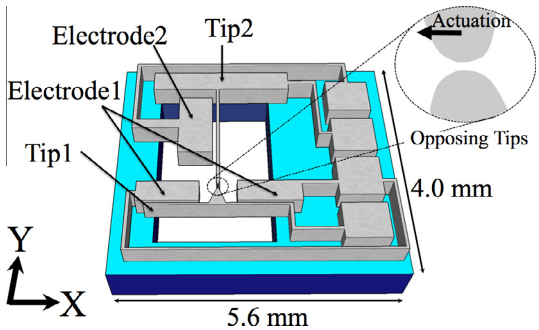

Fig. 1. Schematic representation of the proposed MEMS device in which electrodes are integrated for 2-DOF actuation of the opposing tips. The through-hole in the substrate is used for TEM observation of the junction.

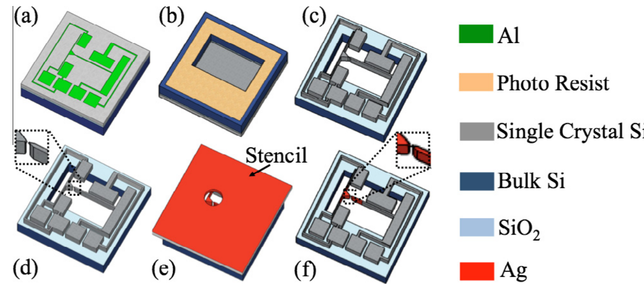

Fig. 2. Schematic representation of the process flow of the MEMS device: (1) Double-sided lithography (a): an Al film was evaporated onto both sides of a SOI wafer. The Al film was patterned using lithography and wet etching on both sides. (2) Back side etching (b): the Si of the back side was etched using the DeepRIE process, and then, the SiO_2 part was removed by wet etching. (3) Frontside etching (c): the Si of the front side was etched using the DeepRIE process, and then, the Al mask was removed by wet etching. (4) Forming opposing tips (d): the Si bridge was etched and sharpened by FIB. (5) Ag evaporation (e): the entire MEMS device was covered except for the tip apexes (f).

matter can be transferred from one tip to the other during short-range sliding [15].

Here, we developed an alternative approach by replacing the conventional piezo-driven actuator/AFM tip with a more compact, versatile and inexpensive micro-electro-mechanical system [16,17]. In our new design, the MEMS, mounted on the TEM holder, integrates 2D electrostatic actuators (XY), enabling the “push and slide” of a movable tip toward a fixed one. A 300 nm gap is formed by FIB before depositing the nano-lubricant (silver in this study) using a shadow-mask technique. Contacting between two silver asperities in UHV leads to the formation of a nanojunction by cold-welding, with a commensurate interface. Junctions with a diameter range between 2.4 and 13.6 nm were obtained. Based on the results, a proportional coefficient, which constitutes the frictional coefficient, was calculated as the quotient of the shear force and the cross-sectional area. The proportional coefficient increased suddenly near sizes of several nanometers.

2. Experimental

2.1. MEMS device principle

A silver nanojunction is formed in-situ in TEM by a cold-welding process between two single silver asperities that are located on two opposing tips composed of silicon. One of those tips is fixed, and the other one can be actuated in two directions, called X and Y as dipicted in Fig. 1. Actuating in the X-direction allows contact between the silver asperities, while a slow elongation process leads to the formation of a single silver nanojunction. The elongation opens an observation window between the thick silicon tips, enabling the electron beam to be transmitted through the silver nanojunction. The sliding process is performed on the movable tip via another electrostatic actuator in the Y-direction, leading to shear deformation of the silver nanojunction. The behavior of the contact area (nanojunction) is monitored and analyzed using real-time video (30 frames/s).

2.2. Fabrication process of MEMS device

Fig. 2 presents the process flow of the MEMS device. The MEMS device was constructed from an SOI wafer with a top 80 μm thick silicon layer. First, the frontside structures were patterned on a sacrificial alumina thin film, passivated with photoresist, and maintained for a final front-side etching at the end of the process. The back side was first etched by plasma (DRIE) to create an open area for the electron beam and to define the final suspended structures on the front side. The buried oxide was wet etched in BHF after the backside etching. Removing the passivation resist on the front side revealed the previous Al patterns on the front side, which were finally etched by plasma (DRIE), leading to suspended structures on the backside opened area. The minimum gap between the electrostatic actuators was typically 3 μm. A compromise was found between the mechanical rigidity of the MEMS and the springs to allow a displacement of approximately 300 nm in the X-direction and a few 100 nm in the Y-direction. The silicon opposing tips were still connected (as designed) even when suspended. We used a focused ion beam (FIB) to separate these silicon tips with a gap of typically 300 nm. Finally, silver was evaporated locally on the separated silicon tips through a shadow mask from the backside of the MEMS, which ensured that the sidewalls were covered with a 30 nm thick silver film within the 300 nm gap.

2.3. Detection method of shear displacement, force, true shear stress and engineering shear strain

The shear force was calculated from two values of displacement: (1) The displacement before formation of the junction, where we actuated the basis of the tip before forming the junction and measured the displacement of the tip of the nanoprobe by TEM, and (2) The displacement after forming the junction, where we similarly actuated the basis of the tip after forming the junction and measured the tip displacement using TEM. The displacement decreased due to the stiffness of the junction. The shear force was calculated as the product of the stiffness of the arm (2.1 N/m) and the difference between the displacement before and after contact formation.

The true shear stress and the engineering shear strain were calculated by monitoring the diameter of the junction. We identified the shortest distance between two sides of the contact as the smallest cross-sectional area and called this distance the “transversal line”. The diameter of the junction corresponds to the length of the transversal line. The cross-sectional area was calculated using

$$A = \pi(d/2)^2 \quad (1)$$

where A is the cross-sectional area and d is the diameter of the junction [the shape of the junction was mentioned in S1 of supplementary data]. The true shear stress was calculated as the quotient of the shear force and the cross-sectional area of the junction as given by Eq. (2)

$$P = F/A \quad (2)$$

where P is the true shear stress, F is the shear force. The engineering shear strain was calculated using Eq.(3). The conventional equation to obtain the engineering shear strain is given by the quotient of the